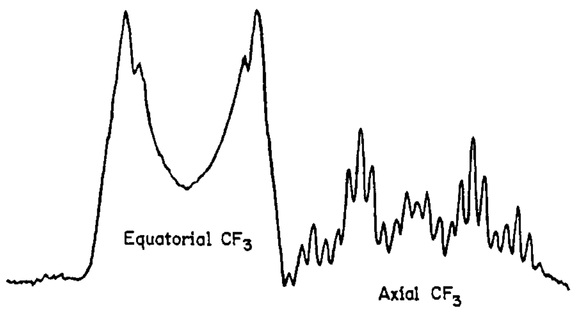

Figure 2. ^{19}F NMR spectrum of CF$_3$ in (CF$_3$PCF$_2$)$_3$, on the XL100 instrument. The XL200 and WM500 instruments show the axial and equatorial patterns farther apart, but with no improvement in resolution. For equatorial CF$_3$, δ = 45.00 and the distance between maxima is 86 s^{-1}. For axial CF$_3$, δ = 46.64, ${}_2J_{FCP}$ = 76 s^{-1}, ${}_3J_{FCPCF}$ = 31.1 s^{-1}, and ${}_5J_{FCPCF}$ = 7.70 s^{-1}.

pression of F against phosphorus lone-pair electrons having mostly 3s character.

The unique CF$_2$ group (between the equatorial CF$_3$ groups) shows an AB spectrum as expected, with remarkably different branches. Upfield (δ = 102.0) there is a clean doublet of triplets: ${}_2J_{FCF}$ = 305.3; ${}_3J_{FCP}$ = 101. Downfield (δ = 86.0; ${}_2J_{FCP}$ confirmed as 304.9) there is only a doublet of broad peaks (half-height width 75 s^{-1}), presumably containing triplets for ${}_3J_{FCP}$ < 35. In the WM500 spectrum, I_o/I_i = 0.92, as observed.

The other CF$_2$ groups show a similar axial–equatorial difference—upfield, δ = 88.38 (${}_2J_{FCF}$ = 364; ${}_3J_{FCP}$ = 139, with minor complexity); downfield, δ = 83.70 (${}_2J_{FCF}$ = 360; secondary ${}_2J$ = 200)—again with peaks broad enough (half-height width 60) to cover a small ${}_3J_{FCP}$. The I_o/I_i ratios (XL200, 0.40; WM500, 0.78) are the same as in the upfield branch. The secondary ${}_2J$ is far larger than would be expected for FCPCF coupling between CF$_2$ groups. The ultimate theoretical analysis here may not be feasible without details covered by the broad peaks.

The ^{31}P spectrum of the trimer could not be resolved: a very broad mound (half-height width 140), with δ = −6.2 (downfield from H$_3$PO$_4$).

The Compound MePCP

The new compound CH$_3$(CF$_3$)PCF$_2$P(CF$_3$)CHF$_2$ ("MePCP") was obtained in 25% yield from the reaction of 2.46 mmol of (CF$_3$)$_2$PH with 2.34 mmol of Zn(CH$_3$)$_2$ (both about 92% consumed) during 11 h at 50 °C in a 22-mL reaction tube that had been washed with dilute aqueous HF and vacuum baked. The yield of (CF$_3$PCF$_2$)$_2$ was only 8% and of the trimer, somewhat less. The purest sample of MePCP from this process contained 12% trimer; with correction for this, the vapor-phase molecular weight was 318 (calculated 316). The volatility is 1.5 mm at 0 °C and 8.4 mm at 26.6 °C; the estimated boiling point is 140 °C if the Trouton constant is 21.6 eu.

The ^{1}H NMR spectrum clearly showed a 3:4 ratio of the diastereomers, respectively at δ = 6.4844 (${}_3J_{HCF}$ = 50.7; ${}_2J_{HCP}$ = 6.70) and δ = 6.4503 (${}_3J_{FCP}$ = 50.7; ${}_2J_{HCP}$ = 7.00). The CH$_3$ spectrum (δ = 1.31; ${}_2J_{HCP}$ = 5.1) showed no resolution of the diastereomers.

The ^{19}F NMR spectrum showed the component groups just in the regions expected on the basis of earlier experience with the same groups. The doublet of multiplets at δ = 49.7 (${}_2J_{FCP}$ = 71) belongs to CF$_3$ in the CF$_3$PCHF$_2$ group, and δ = 55.9 (${}_2J_{FCP}$ = 72) is correct for the CH$_3$PCF$_3$ group. In the connecting PCF$_2$P group, F appears at δ = 101, as an AB spectrum in which the A and B parts have superposed inner branches, even in the WM500 spectrum; ${}_2J_{FCF}$ might be near 60. The CHF$_2$ group shows well-separated A and B branches, only the latter of which is easily sorted out into the diastereomeric components: δ range 115.7–119.9.

For still further confirmation of the formula, an authentic synthesis of MePCP was performed, beginning with a methoxide-catalyzed methanolysis of (CF$_3$PCF$_2$)$_2$ to MeOPCP, convertible to ClPCP and so by action of Zn(CH$_3$)$_2$ to MePCP. The product has the same NMR spectra as the MePCP here described. A fuller description of MePCP and the other PCP compounds mentioned here, with a fuller analysis of their NMR spectra and the further consequences of dimer methanolysis, is planned for future publication.

Acknowledgment. Gratitude is due to the operators of the XL200-FT and WM500-FT NMR spectrometers and to Dr. K. L. Servis for critical and constructive suggestions concerning NMR spectra.

Registry No. (CF$_3$)$_2$PH, 460-96-8; Zn(CH$_3$)$_2$, 544-97-8; CF$_3$P=CF$_2$, 72344-34-4; (CH$_3$)$_3$N, 75-50-3; *cis*-(CF$_3$PCF$_2$)$_2$, 86350-48-3; *trans*-(CF$_3$PCF$_2$)$_2$, 86350-49-4; (CF$_3$PCF$_2$)$_3$, 86350-50-7; CH$_3$(CF$_3$)PCF$_2$P(CF$_3$)CHF$_2$ (isomer 1), 86350-51-8; CH$_3$(CF$_3$)PCF$_2$P(CF$_3$)CHF$_2$ (isomer 2), 86350-52-9; diborane, 19287-45-7.

Contribution from the Department of Chemistry,
University of California, Riverside, California 92521

Synthesis and Characterization of Tetramethylammonium Superoxide

DONALD T. SAWYER,* THOMAS S. CALDERWOOD, KENNETH YAMAGUCHI, and CHARLES T. ANGELIS

Received December 2, 1982

The experimental conditions for the synthesis (and isolation) of tetramethylammonium superoxide [(Me$_4$N)O$_2$] from KO$_2$ and (Me$_4$N)OH·5H$_2$O in liquid ammonia have been optimized. The isolated solid salt has an assay of greater than 99.5% purity but a magnetic susceptibility that indicates only 10–20% of the molecules are paramagnetic and monomeric. In dry acetonitrile a 4 mM solution of (Me$_4$N)O$_2$ initially is 25% monomeric; after 2.5 days it has increased to 90% monomeric at the expense of the dimer, [(Me$_4$N)$_2$O$_2$]$_2$. Dissociation of the dimer is accelerated by trace levels of water (5–10 mM). The absorption spectrum of the monomer in dry acetonitrile has a single band that is characteristic of O$_2^-$ (λ_{max} 257 nm (ϵ 10.1/mM^{-1} cm^{-1})). The diamagnetic dimer, [(Me$_4$N)O$_2$]$_2$, has a single absorption band at 289 nm (ϵ 11.6 mM^{-1} cm^{-1}) (dimer), and there is an isosbestic point at 278 nm (ϵ 5.0 mM^{-1} cm^{-1}) (monomer). The monomeric species has been characterized in the solid phase and in aprotic solvents by ESR, infrared, and Raman spectroscopy and by electrochemistry.

Since the observations that superoxide (O$_2^-$) is a respiratory intermediate[1] and an effective nucleophile in aprotic media,[2,3] there has been growing interest in the chemistry of O$_2^-$. At present, the most effective methods for the in situ generation of O_2^- in aqueous solutions are via pulse radiolysis of O_2 in the presence of formate ion[4] and UV flash photolysis of H_2O_2.[5] Both methods produce transient concentrations of O_2^- (<0.5 mM for less than 1 s), but the generation system must be free of reactive substrates.

With aprotic media (Me_2SO, DMF, MeCN, or pyridine) O_2^- concentrations up to 10 mM can be electrosynthesized by controlled-potential reduction of molecular oxygen.[6] However, the process is tedious, the product solutions contain supporting electrolyte, and the half-life of O_2^- in the solutions is less than 7 h.

Although solid KO_2 is available from several sources, its purity is limited to 96% (with K_2O_2 and KOH the main impurities) and it has low solubilities in aprotic solvents (1.3 mM in Me_2SO, 0.33 mM in DMF, and 0.016 mM in MeCN). The latter limitation can be circumvented by the use of 18-crown-6 ether.[7] A somewhat more soluble salt, NaO_2, can be prepared from Na_2O_2 and O_2 in a pressurized bomb (450 °C and 280 atm); the isolated material has a purity of approximately 92%.[8,9]

The preparation of tetramethylammonium superoxide $(Me_4N)O_2$ from KO_2 and $Me_4NOH{\cdot}5H_2O$ via a solid-phase metathesis reaction and subsequent extraction into liquid ammonia was first described in 1964:[10]

$$\begin{aligned} &11KO_2(s) + (MeN)OH{\cdot}5H_2O(s) \rightarrow \\ &\quad (Me_4N)O_2(s) + 5KO_2H(s) + 6KOH(s) + 5O_2 \xrightarrow{NH_3} \\ &\qquad (Me_4N)O_2 + 11KOH(s) + 7^1/_2O_2 \end{aligned} \tag{1}$$

However, the absence of specific experimental details in this early report has prompted new investigations to determine the optimum synthetic conditions.[10]

The present paper summarizes the optimization of the synthetic procedure for the preparation of pure $(Me_4N)O_2$. The isolated salt, which has been characterized in terms of its electrochemical, spectroscopic, and magnetic properties, provides a unique soluble source of superoxide ion. In pure anhydrous solvents $(Me_4N)O_2$ solutions are stable for several days.

Experimental Section

Reagents. The primary reagents for the synthesis of $(Me_4N)O_2$ were KO_2 (96%) from Alfa and $(Me_4N)OH{\cdot}5H_2O$ from Southwest Analytical. Anhydrous ammonia (Matheson) was used for the extraction, and the synthetic process was protected from atmospheric moisture with ultrapure nitrogen (Linde Gas Co.) and Type 4A molecular sieves (MCB). The solvents that were used for the characterization of the isolated $(Me_4N)O_2$ were "Distilled-in-Glass" grade from Burdick and Jackson and included acetonitrile (MeCN), dimethyl sulfoxide (Me_2SO), dimethylformamide (DMF), and pyridine. The MeCN solvent was dried further by passage through a column of Woelm N Super I activated alumina immediately prior to its use (this reduced the level of H_2O to <1 mM).[11]

Tetramethylammonium perchlorate and tetraethylammonium perchlorate from Southwestern Analytical were dried on a vacuum line prior to use as supporting electrolytes in the electrochemical experiments.

Synthesis Procedure. In a Vacuum Atmospheres glovebox, KO_2 (70 g (1 mol)) and $Me_4NOH{\cdot}5H_2O$ (10 g (0.055 mol)) were ground separately in mortars to fine powders prior to their addition to a 500-mL round-bottom flask. Approximately 40 mL of 3-mm diameter glass beads was added to the flask as a mixing and grinding agent. The round-bottom flask was sealed with a Rota-evaporator top and moved from the glovebox to the Roto-evaporator. The dry solid mixture was rotated under vacuum for at least 3 days and returned to the glovebox. Next, the contents were transferred to a glass filtration cup and then placed in a specially designed Soxhlet extractor. A cold-finger condenser was mounted on the top of the Soxhlet extractor. The stopcock of the condenser was closed, and the bottom opening of the Soxhlet extractor was sealed with a glass stopper prior to transfer of the assemblage to a fume hood. The cold-finger condenser was connected through a two-way stopcock to compressed-gas cylinders of ammonia and ultrapure nitrogen. The stopcock allowed selection between a mixture of both gases and pure nitrogen for passage through the system. A Type 4A molecular-sieve trap was placed in the gas line to reduce the level of residual moisture. This trap was immersed in an ice-water bath to cool the gases prior to passage to the cold finger. With a slight flow of nitrogen through the system to minimize the opportunity for atmospheric water contamination, the glass stopper on the bottom of the Soxhlet extractor was replaced with the collection flask. The sidearm of the collection flask was vented through a mineral-oil bubbler, which prevented the back-diffusion of water into the system. Next, the reservoir of the cold finger was filled with a dry ice/acetone slurry, and the two-way stopcock was switched to allow the passage of both nitrogen and ammonia into the system (the condensed ammonia extracted $(Me_4N)O_2$ from the glass extraction cup into the collection flask). A slight flow of nitrogen was necessary to prevent the development of subatmospheric pressures within the system as the ammonia condensed on to a liquid. After three extractions of the solution from the Soxhlet extractor chamber into the collection flask, the flow of ammonia was shut off and the two-way stopcock was switched to allow just nitrogen to flow through the system. The collection flask was removed and closed with a glass stopper. The residual liquid ammonia was allowed to evaporate through the sidearm via the mineral-oil bubbler. After the ammonia was completely removed, the collection flask was transferred to the glovebox. The $(Me_4N)O_2$ in the flask (about 4.6 g) was transferred to a preweighed glass container.

The isolated $(Me_4N)O_2$ was assayed for base content, after dissolution in distilled water ($2O_2^- + 2H_2O \rightarrow H_2O_2 + 2OH^-$), by titration with HCl. The yield of H_2O_2 from solid $(Me_4N)O_2$ was determined by dissolution in water, followed by the addition of H_2SO_4, KI, and ammonium molybdate, and titration with $Na_2S_2O_3$. The Me_4N^+ content of $(Me_4N)O_2$ was determined, after dissolution in $Me_2SO\text{-}d_6$, by proton NMR (calibration was accomplished with weighed quantities of $(Me_4N)Cl$). On the basis of these assays, the isolated lots of $(Me_4N)O_2$ had purities that ranged from 85% to 99%.

Instrumentation. A three-electrode potentiostat (Princeton Applied Research Model 173 potentiostat/galvanostat with a Model 175 universal programmer and Model 179 digital coulometer) was used for the cyclic voltammetric and controlled-potential electrolysis experiments. Cyclic voltammograms were recorded on a Houston Instruments Series 200 recorder. The scans were initiated at the rest potential of each solution.

The Leeds & Northrup electrochemical cell was equipped with a Beckman platinum-inlay working electrode (area 0.23 cm^2) or a glassy-carbon-inlay working electrode (area 0.11 cm^2), a platinum-flag auxiliary electrode, and an Ag-AgCl reference electrode filled with aqueous tetramethylammonium chloride solution and adjusted to 0.000 V vs. SCE. The latter was contained in a Pyrex tube with a soft-glass cracked tip; this electrode was placed inside a Luggin capillary. For controlled-potential electrolysis, a platinum-mesh working electrode or sheets of graphitized carbon and a platinum-mesh auxiliary electrode were employed. All of the electrochemical electrodes and degassing apparatus were contained inside a Brinkmann electrochemical cell equipped with an O-ring seal. For the electrosynthesis of O_2^- in MeCN, a double-bridged H-cell was used (which included a center compartment that could be flushed with supporting electrolyte).

Cary Model 17D and Model 219 spectrophotometers were used for the UV-visible spectrophotometric measurements. The magnetic susceptibility measurements for solid $(Me_4N)O_2$ were made by the

---

(1) Knowles, P. F.; Gibson, J. F.; Pick, F. M.; Bray, R. C. *Biochem. J.* **1969**, *111*, 53.

(2) Dietz, R.; Forno, A. E. J.; Larcombe, B. E.; Peover, M. D. *J. Chem. Soc. B* **1970**, 816.

(3) Merritt, M. V.; Sawyer, D. T. *J. Org. Chem.* **1970**, *35*, 2157.

(4) Czapski, G. *Annu. Rev. Phys. Chem.* **1971**, *22*, 171.

(5) Nadezhdin, A. D.; Dunford, H. B. *J. Phys. Chem.* **1979**, *83*, 1957.

(6) Sawyer, D. T.; Roberts, J. L., Jr. *J. Electroanal. Chem.* **1966**, *12*, 90.

(7) Valentine, J. S.; Curtis, A. B. *J. Am. Chem. Soc.* **1975**, *97*, 224.

(8) Stephanou, S. E.; Schechter, W. H.; Argersinger, W. J., Jr.; Kleinberg, J. *J. Am. Chem. Soc.* **1949**, *81*, 1819.

(9) Stephanou, S. E.; Seyh, J. S., Jr.; Kleinberg, J. *Inorg. Synth.* **1953**, *4*, 82.

(10) McElroy, A. D.; Hashman, J. S. *Inorg. Chem.* **1964**, *3*, 1798.

(11) Kiesele, H. *Anal. Chem.* **1980**, *52*, 2230.

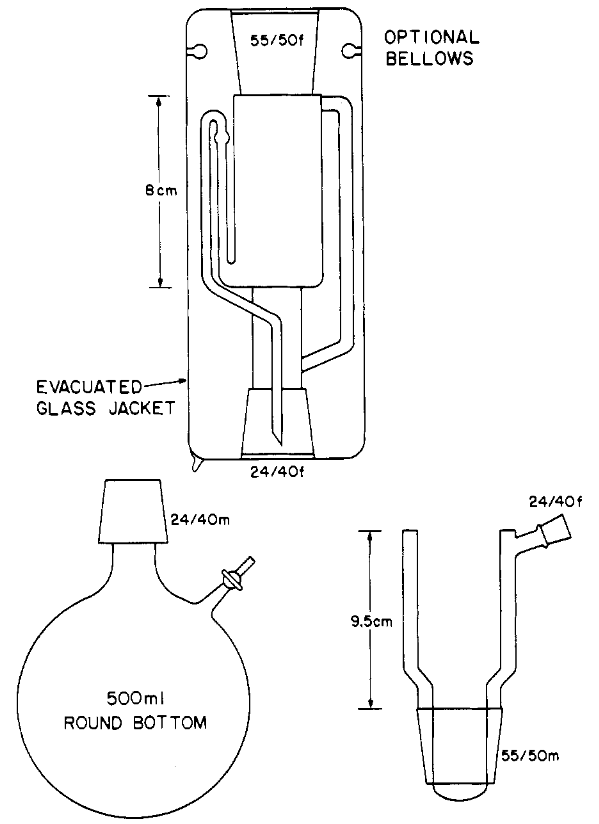

Figure 1. Special Soxhlet apparatus for the extraction with liquid ammonia of $(Me_4N)O_2$ from the reaction mass of its solid-state metathesis (20:1 mole ratio of KO_2 and $(Me_4N)OH·5H_2O$). A glass cup with a fritted-glass bottom is used to hold the solid material and is placed inside the upper vacuum-jacketed section.

Faraday method on a Cahn Model 2000 balance at room temperature (25 °C) and by the Gouy method at room temperature and at 8 °C.

Infrared measurements were made by use of Nujol mulls in a Perkin-Elmer Model 283 spectrophotometer. The Raman spectra were obtained with a Spex Industries Ramalog 6 laser-Raman spectrometer with customized optics and detection; the ESR spectra were measured with a Bruker Model ER 200 spectrometer.

Results

Synthesis. Although the synthetic procedure for the preparation of $(Me_4N)O_2$ that is outlined by McElroy and Hashman[10] appears straightforward, its direct application results in poor yields and an impure product. For a successful synthesis, the starting materials, KO_2 (>95% pure) and $Me_4NOH·5H_2O$ (>99% pure), must be pure and dry and must be ground to a fine powder in an inert atmosphere prior to their combination.

The reaction stoichiometry of eq 1 appears reasonable, but poor yields and impure products result unless a KO_2:$Me_4NOH·5H_2O$ mole ratio of at least 18 is used. The excess KO_2 acts as an essential dehydrating agent and drives the solid-phase metathesis reaction to completion. The reaction proceeds to a limited degree as a static mixture. However, the extent and rate of the reaction are maximized by grinding the mass with glass beads for at least 3 days in a round-bottomed flask.

Because the side-delivery arm on a conventional Soxhlet extractor is prone to become clogged, this has been redesigned with a larger diameter tube (Figure 1). The traditional cellulose collection cup has been replaced with a large glass cup with a fritted-glass bottom. *Warning*! Use of a paper collection cup has resulted in several vigorous spontaneous combustions. The essential ingredients are residual KO_2 (in the solid mass after extraction), cellulose, and exposure to the moisture in ambient air. Combination of solid KO_2 and powdered cellulose in a beaker that is left exposed to ambient air will result in spontaneous combustion (see footnote 8 of a recent paper for another cautionary warning[12]).

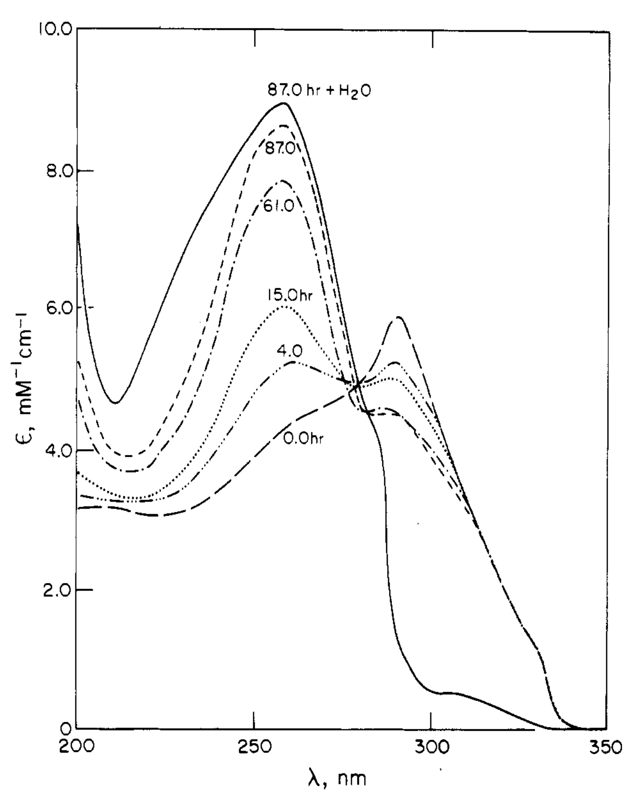

Figure 2. Absorption spectra for 3.6 mM $(Me_4N)O_2$ in dry MeCN (<1 mM H_2O) as a function of the age of the solution (hours after preparation from solid $(Me_4N)O_2$). The molar absorptivities are relative to the number of O_2^- centers per liter (mM). The addition of H_2O (50 mM) to the sample cuvette causes the 290-nm band to disappear.

Spectroscopy. The UV-visible absorption spectra of $(Me_4N)O_2$ in dry acetonitrile as a function of time after preparation are illustrated by Figure 2. The isosbestic point at 278 nm has a molar absorptivity of 5.0 ± 0.5 mM^{-1} cm^{-1} and provides a convenient means to assay solutions for their total concentration of the apparent two forms of $(Me_4N)O_2$. The absorbance at 278 nm in Figure 2 indicates that there is a degradation of approximately 5% of the $(Me_4N)O_2$ in a sealed spectrophotometer cell during a period of 3.6 days. Analysis of the data of Figure 2 yields approximate values for the molar absorptivities of the two forms of $(Me_4N)O_2$. The species with a maximum at 257 nm has a value of 10.1 ± 1.0 mM^{-1} cm^{-1} (assumed to be monomeric $(Me_4N)O_2$), and that at 289 nm has a value of 5.8 ± 0.6 mM^{-1} cm^{-1} as a monomer but 11.6 ± 1.0 mM^{-1} cm^{-1} if it is assumed to be a dimer, $[(Me_4N)O_2]_2$.

Figure 3 illustrates the effect on the absorption spectra of $(Me_4N)O_2$ when a stock solution of $(Me_4N)O_2$ (4.7 mM) in dry MeCN is diluted with MeCN that contains 5 mM H_2O. As the ratio of H_2O per $(Me_4N)O_2$ exceeds 4, the dimeric form is converted to monomer, the isosbestic point at 278 nm (Figure 2) is shifted to 266 nm (ϵ 5.1 ± 0.5 mM^{-1} cm^{-1}), and the absorption maximum for the monomer is shifted to 253 nm.

When a 5.2 mM solution of $(Me_4N)O_2$ in MeCN is diluted 10-fold with pure H_2O (0.1 M $(Me_4N)OH·5H_2O$), the resulting solution has a single absorption band at 257 nm (ϵ 6.7 mM^{-1} cm^{-1}). Because of dilution and the possibility of ul-

---

[12] Foote, C. S.; Shook, F. C.; Abakerli, R. A. *J. Am. Chem. Soc.* **1980**, *102*, 2503.

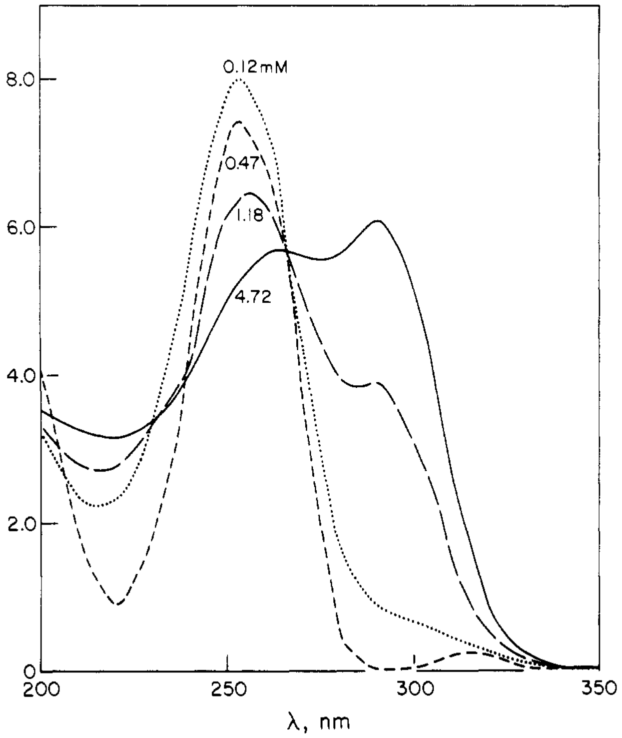

Figure 3. Absorption spectra for 4.7 mM $(Me_4N)O_2$ in dry MeCN (<1 mM H_2O) and for solutions prepared by its dilution (4-fold, 10-fold, and 40-fold) with MeCN that contained 5 mM H_2O.

tratrace levels of metals in the Milli-Q water and the $(Me_4N)OH{\cdot}5H_2O$, this is believed to be a lower limit for the molar absorptivity of O_2^- in aqueous solution. Other experiments have given values from 5.0 to 7.5 mM^{-1} cm^{-1}; we suspect that the true value is the same as that observed in MeCN (ϵ 10.1 mM^{-1} cm^{-1}).

The surprising result for the 0.5 mM solutions of $(Me_4N)O_2$ in 90% H_2O (0.1 M $(Me_4N)OH$) and 10% MeCN is their stability; after 15 h the concentration decreases about 10–15%. Even with only 10^{-6} M $(Me_4N)OH$ present, such solutions have a half-life of about 1 h. However, attempts to prepare aqueous solutions (0.1 M $(Me_4N)OH$) from solid $(Me_4N)O_2$ result in rapid and complete decomposition. Hence, the presence of 10% MeCN is necessary.

When Me_2SO is saturated with KO_2, the resulting solution contains 1.3 mM O_2 (on the basis of its voltammetric peak current) and has an absorption maximum at 257 nm (ϵ 8.0 mM^{-1} cm^{-1}). Electrosynthesis of O_2^- in MeCN by controlled-potential coulometric reduction of O_2 is 27% efficient at a platinum-gauze electrode and is 67% efficient at a graphitized-carbon electrode. The resulting product solutions have an absorption maximum at 252 nm (ϵ 6.5 mM^{-1} cm^{-1}). These and previous spectrophotometric measurements of superoxide in a variety of solvents are summarized in Table I.[13-17] Attempts to determine a molar absorptivity of O_2^- by dissolving KO_2/18-crown-6 ether in acetonitrile have been unsuccessful due to the extremely low solubility of the system.

An early Raman study[18] of solid KO_2 reports a value of 1145 cm^{-1} for the O–O vibration. A subsequent investigation[19] of NaO_2 in Na_2O_2 gives a value of 1141 cm^{-1} for the superoxide group and values of 739 and 794 cm^{-1} for the peroxide stretch.

Table I. UV Absorption of Superoxide Ion from Several Sources in Various Media

source	media	λ_{max}, nm	ϵ, mM^{-1} cm^{-1}	ref
pulse radiolysis of O_2 in aqueous formate	H_2O	240	1.95	13
pulse radiolysis of O_2 in aqueous formate	H_2O	245	2.35	14
controlled-potential electrolysis of O_2	MeCN	250	2.58	15
coulometric reduction of O_2	MeCN	255	1.46	16
controlled-potential electrolysis of O_2	MeCN	252	6.5 ± 1.0	this work
$(Me_4N)O_2$ (4 mM)	MeCN	257	10.1 ± 1.0	this work
$[(Me_4N)O_2]_2$ (1.5 mM)	MeCN	289	11.6 ± 1.0 (dimer)	this work
$(Me_4N)O_2$ (0.5 mM)	90%:10% H_2O/MeCN (0.1 M $(Me_4N)OH$)	257	6.7 ± 1.0	this work
KO_2/18-crown-6 ether	Me_2SO	250	2.69	17
KO_2 (1.3 mM)	Me_2SO	257	8.0 ± 1.0	this work

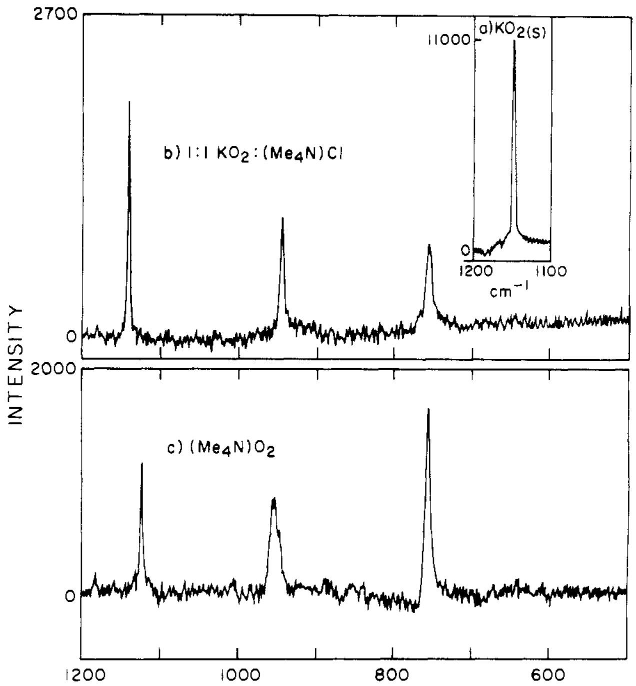

Figure 4. Raman spectra for solid samples of $(Me_4N)O_2$ and of 50:50 wt/wt mixture of $(Me_4N)Cl$ and KO_2. The inset illustrates the emission line for a pure sample of solid KO_2 (96% pure). The same sample tubes and amount of sample were used for each spectrum. (The magnetic moment for this lot of $(Me_4N)O_2$ indicated that about 25–35% of the molecules were paramagnetic and monomeric.)

Matrix isolation of O_2^- in KCl yields a Raman line at 1145 cm^{-1}.[20] Figure 4 illustrates the Raman spectra for KO_2 (1144 cm^{-1}), for a 50:50 wt/wt mixture of KO_2 and $(Me_4N)Cl$, and for $(Me_4N)O_2$. The emission line at 1123 cm^{-1} for the last is assigned to the superoxide symmetrical stretch; the remaining lines at 955 and 760 cm^{-1} are due to the Me_4N^+ group. On the basis of the relative intensities of the O_2^- line

---

(13) Rabani, J.; Nielson, S. O. *J. Phys. Chem.* **1969**, *73*, 3736.
(14) Bielski, B. H. J. *Photochem. Photobiol.* **1978**, *28*, 645.
(15) Fee, J. A.; Hildenbrand, P. G. *FEBS Lett.* **1974**, *39*, 79.
(16) Ozawa, T.; Hanaki, A.; Yamamoto, H. *FEBS Lett.* **1977**, *74*, 99.
(17) Kim, S.; Di Cosimo, R.; San Filippo, J., Jr. *Anal. Chem.* **1979**, *51*, 679.
(18) Creighton, J. A.; Lippincott, E. R. *J. Chem. Phys.* **1964**, *40*, 1779.
(19) Evans, J. C. *J. Chem. Soc., Chem. Commun.* **1969**, 682.
(20) Holzer, W.; Murphy, W. F.; Berstein, H. J.; Rollfe, J. *J. Mol. Spectrosc.* **1968**, *26*, 543.
(21) Green, M. R.; Hill, H. A. O.; Turner, D. R. *FEBS Lett.* **1979**, *103*, 176.
(22) Valentine, J. S.; Tatsuno, Y.; Nappa, M. *J. Am. Chem. Soc.* **1977**, *99*, 3522.

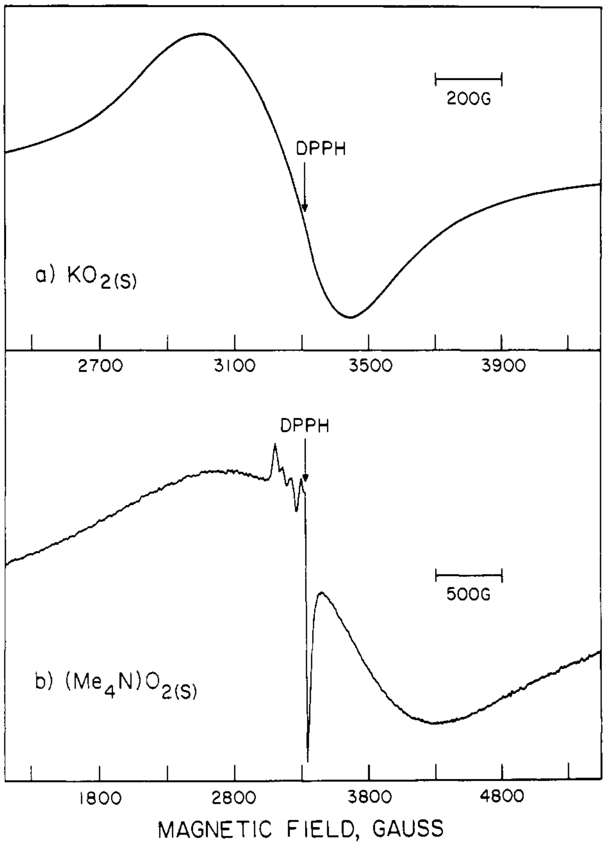

Figure 5. ESR spectra for solid samples of KO_2 (96% pure) and pure $(Me_4N)O_2$ at 77 K.

to the Me_4N^+ lines for the $KO_2/(Me_4N)Cl$ mixture and for $(Me_4N)O_2$, only about 25% of the O_2^- for the latter is present as a monomeric species with a Raman activity analogous to that of KO_2. The infrared spectrum of $(Me_4N)O_2$ (as a Nujol mull) has absorption bands at 1491 (m), 1410 (m), 922 (w), 820 (w), and 780 (w) cm^{-1}. The last two may be due to a peroxide-like vibration for the dimeric form of $(Me_4N)O_2$.

Figure 5 illustrates the ESR spectra at 77 K for solid KO_2 and $(Me_4N)O_2$. The hyperfine splittings on the broad spectrum of the latter are characteristic of dilute solutions of O_2^- in DMF glasses and of $(Me_4N)O_2$ in Me_2SO glasses. The broadness of the spectra indicates dipolar coupling between nearby O_2^- molecules. The hyperfine structure on the spectrum of Figure 5b is due to isolated O_2^- ions; these exhibit g values that are consistent with their spin Hamiltonian.[23] A rough comparison of the width and power settings for the KO_2 and $(Me_4N)O_2$ ESR spectra of Figure 5 indicates that about 10%–25% of the latter material is paramagnetic. Table II summarizes the ESR parameters for $(Me_4N)O_2$ and other sources of O_2^- in solid and solution phases.[16,21-24] Dilution and the presence of electrolytes narrow the line widths.

Table II

ESR g Values for $(Me_4N)O_2$

concn, mM, or additive	DMF $g_\parallel$	DMF $g_\perp$	Me_2SO $g_\parallel$	Me_2SO $g_\perp$
A. Pure $(Me_4N)O_2$				
10	2.14	2.00	2.14	2.00
5	2.11 (350)	2.00 (50)	2.11	2.02
3	2.15	2.00	2.10	2.00
1	2.00 (50)		2.10	2.00
solid	2.00 (2.5 kG)			
B. 5 mM $(Me_4N)O_2$ (Effect of 0.5 M Additives)				
H_2O	2.11 (73)	2.00 (20)	2.14	2.00
MeOH	2.09 (33)	2.00 (10)	2.07	2.00
$(Me_4N)ClO_4$	2.15 (61)	2.00 (24)		
$(Et_4N)ClO_4$	2.13 (61)	2.00 (12)	2.10	2.00
$(Pr_4N)ClO_4$	...	2.00 (24)	2.10	2.00
$(Bu_4N)ClO_4$	...	2.00 (163)	2.11	2.00
$(Me_4N)BF_4$	2.16 (122)	200 (24)	2.15	2.00
$(Et_4N)BF_4$		2.00 (20)	2.11	2.00

ESR g Values for Other Sources of Superoxide in Various Media

	media	$g_\parallel$	$g_\perp$	ref
O_2^- (electro-synthesized)	MeCN (0.1 M $(Et_4N)ClO_4$)	2.083	2.008	16
O_2^- (electro-synthesized)	DMF (0.1 M $(Et_4N)ClO_4$)	2.22	2.002	21
KO_2	18-crown-6 ether, Me_2SO	2.11	2.01	22
KO_2	Me_2SO (0.1% H_2O)	2.12		24
KO_2	H_2O	2.065		24

Table III. Electrochemical Parameters for the Oxidation of O_2^- at Platinum and at Glassy-Carbon Electrodes and Solubilities of KO_2 in Several Aprotic Solvents That Contain 0.1 M Tetraethylammonium Perchlorate

A. Electrochemical Parameters for O_2^- (Produced by Electroreduction of O_2; Scan Rate 0.1 V s^{-1})

solvent	$i_{p,a}$, $\mu A\ mM^{-1}$ 0.23 cm^2 Pt, 0.1 V s^{-1}	$i_{p,a}$, $\mu A\ mM^{-1}$ 0.11 cm^2 C, 0.1 V s^{-1}	$10^5 D_{O_2^-}$, $cm^2\ s^{-1}$
MeCN	75 ± 4	35 ± 4	1.49
DMF	49 ± 2	23 ± 2	0.63
Me_2SO	37 ± 2	17 ± 2	0.36

B. Solubility of KO_2 at 25 °C

solvent	$[O_2^-]_{satd}$, mM	0.1 M $(Et_4N)ClO_4$ $[O_2^-]_{satd}$, mM
MeCN	0.016	0.016
DMF	0.32	0.40
Me_2SO	1.3	5.4

Magnetic Properties. The molar magnetic susceptibilities, χ_m, of solid KO_2 (96% pure) and $(Me_4N)O_2$ (99.5%) are 15.0 (±0.3) × 10^{-4} and 1.23 (±0.3) × 10^{-4} cgsu, respectively, on the basis of measurements with a Faraday balance at 25 °C. Although these values are not corrected for diamagnetic susceptibilities, they can be converted to approximate magnetic moments, μ (in μ_B) via the relation

$$\mu = 2.824(\chi_m T)^{1/2} \tag{2}$$

This gives values of 1.89 and 0.54 μ_B for KO_2 and $(Me_4N)O_2$, respectively. Thus, only about 9% of the $(Me_4N)O_2$ molecules are in a form with an unpaired electron [(1.23/15.0) × 100 = 8.2%], in contrast to the 100% content of KO_2. When the reaction mass for a preparation of $(Me_4N)O_2$ is exhaustively extracted (more than three passes through the Soxhlet), the isolated material is less pure (50%–95%) and the measured magnetic susceptibilities indicate that about 25%–50% of the $(Me_4N)O_2$ molecules are monomeric with one unpaired electron.

Electrochemistry. Figure 6 illustrates the cyclic voltammetry at a glassy-carbon electrode of oxygen, KO_2, and $(Me_4N)O_2$ in Me_2SO (0.1 M TEAP) and MeCN (0.1 M TEAP) solutions. The peak heights for the oxidation of $(Me_4N)O_2$ indicate that approximately one-third of the freshly dissolved solid is electroactive. The absorption spectrum of such a solution confirms that about one-third of the dissolved $[(Me_4N)O_2]_2$ is monomeric; the dimer is not electroactive at

---

(23) Fee, J. A.; Valentine, J. S. In "Superoxide and Superoxide Dismutases"; Michelson, A. M., McCord, J. M., Fridovich, I., Eds.; Academic Press: New York, 1977; pp 19–60.

(24) Symons, M. C. R. *J. Chem. Soc., Faraday Trans. 1* **1980**, *76*, 1868.

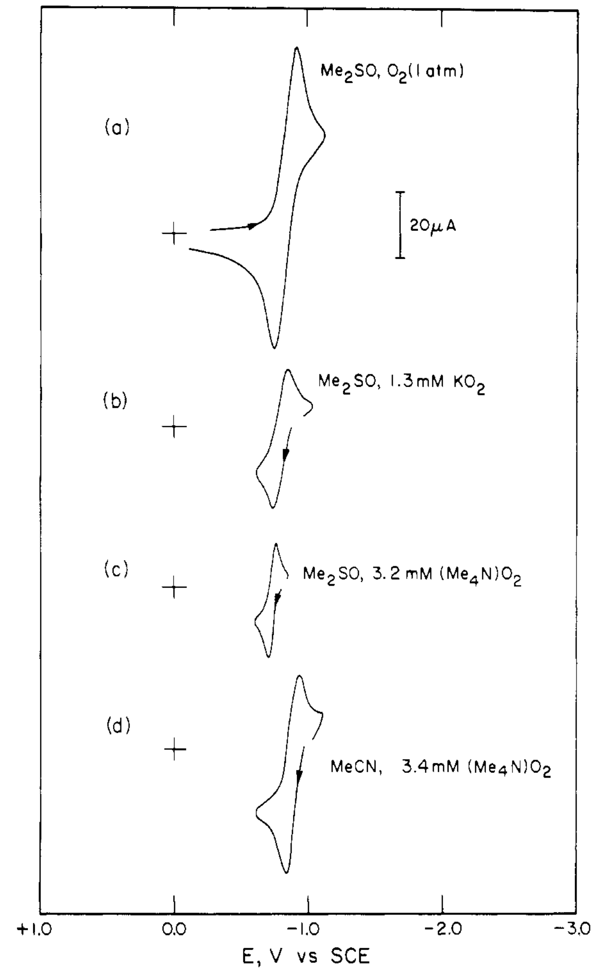

Figure 6. Cyclic voltammograms at a glassy-carbon electrode (area 0.11 cm^2): (a) 2.1 mM O_2 (1 atm) in Me_2SO (0.1 M tetraethylammonium perchlorate (TEAP)); (b) 1.3 mM KO_2 in Me_2SO (0.1 M TEAP); (c) 3.2 mM $(Me_4N)O_2$ in Me_2SO (0.1 M TEAP); (d) 3.4 mM $(Me_4N)O_2$ in MeCN (0.1 M TEAP). Scan rate = 0.1 V s^{-1}.

the anodic peak potential for O_2^- (−0.6 V vs. SCE). Hence, the initial positive scan by linear-sweep voltammetry yields a peak current that represents the concentration of monomeric $(Me_4N)O_2$ (equivalent to free O_2^-). The proportion of free O_2^- increases with time in a manner that is analogous to the spectral changes of Figure 2. Table III summarizes the peak currents in μA (mM O_2^-)$^{-1}$ and the diffusion coefficients for O_2^- in several aprotic solvents. These parameters have been used to ascertain the solubility of KO_2 in Me_2SO, DMF, and MeCN that contains 0.1 M tetraethylammonium perchlorate (Table III).

Discussion and Conclusions

Consideration of the magnetic, Raman, spectrophotometric, and electrochemical data for tetramethylammonium superoxide supports the conclusion that at least 90% of the isolated solid is dimeric, $[(Me_4N)O_2]_2$, with a structure that is essentially diamagnetic. One possibility is a coupling of the unpaired electrons of two $(Me_4N)O_2$ molecules to give $(Me_4N^+)^-O–O–O–O^-(^+NMe_4)$. The weak infrared lines at 820 and 780 cm^{-1} are consistent with such a structure. Furthermore, the reduced intensity of the Raman line for the superoxide vibration of $(Me_4N)O_2$ relative to that observed for solid KO_2 (Figure 4) provides strong support for the conclusion that the major fraction of the $(Me_4N)O_2$ is dimeric with bond formation via radical–radical coupling. Other possible diamagnetic configurations include a diamond array of four oxygen atoms

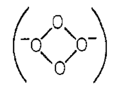

and a tetrahedral array of crossed O–O dumbbells

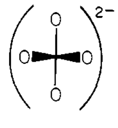

The absence of detectable Raman lines for the dimeric $(O_2)_2^{2-}$ group may be due to the presence of several configurations, weak or disallowed transitions, or thermal exchange and disorder.

The UV spectral changes that are illustrated by Figure 2 are consistent with assignment of the 289-nm band to the dimer and the 253-nm band to the monomer of $(Me_4N)O_2$. Thus, in the solid phase, the material is more than 90% dimeric. When dissolved in dry acetonitrile, it begins to dissociate slowly into the monomeric form. The presence of water accelerates the dissociation process

$$[(Me_4N)O_2]_2 \rightleftharpoons 2(Me_4N)O_2 \xrightarrow[\text{fast}]{H_2O} (Me_4N)O_2(H_2O)_n \quad (3)$$

as well as the rate of decomposition

$$(Me_4N)O_2(H_2O)_n \rightarrow (Me_4N)OH + {}^1/_2H_2O_2 + {}^1/_2O_2 \quad (4)$$

Two recent studies[21,25] have concluded that O_2^- in aqueous media and in aprotic media is coordinated by several (about four) water molecules. Because the UV absorption maximum for dilute $(Me_4N)O_2$ in the presence of excess water in MeCN (Figure 3) is closely related to that for O_2^- in aqueous solutions, a reasonable conclusion is that several water molecules are associated with the monomeric form and serve to stabilize it by such coordination. The shift in the isosbestic point for the dissociation of the dimeric form of $(Me_4N)O_2$ in dry MeCN (278 nm, Figure 2) to 266 nm (Figure 3) for dilute conditions where an excess of H_2O is present probably is due to hydration of the monomeric species:

$$[(Me_4N)O_2]_2 + 8H_2O \rightarrow 2(Me_4N)O_2(H_2O)_4 \quad (5)$$

The electrochemical results indicate that the dimer is not oxidized at −0.5 V vs. SCE. The monomeric species, $(Me_4N)O_2(H_2O)_n$, is indistinguishable from electrosynthesized O_2^- or dissolved KO_2 in the various solvents in terms of its spectroscopy and electrochemistry.

Although the previous evaluations of the molar absorptivity for O_2^- (see Table I) are much smaller than the 10.1 mM^{-1} cm^{-1} value for monomeric $(Me_4N)O_2$, there are reasons to believe that this is the correct value for O_2^- in MeCN and is close to its true value in most solvents. The spectral observations after $(Me_4N)O_2$ in MeCN is diluted 10-fold with a 0.1 M $(Me_4N)OH$ aqueous solution yield a value of 6.7 mM^{-1} cm^{-1}. This is substantially greater than the values observed from the pulse radiolysis generation of O_2^- (1.76 mM^{-1} cm^{-1} and 2.36 mM^{-1} cm^{-1}), which were based on a stoichiometric yield of O_2^-.

The same is true in the case of the evaluations of the molar absorptivity via the electrogeneration of O_2^- in MeCN. The value of 1.46 mM^{-1} cm^{-1} for the generation at a mercury electrode[16] was determined on the basis that the coulometric electrolysis was 100% efficient. The value of 2.58 mM^{-1} cm^{-1} for the generation at a platinum electrode[15] was based on O_2^- concentrations that were determined by the acid-catalyzed release of O_2 in an oxygen-electrode measurement chamber and by double-integration of the EPR intensities for O_2^- at 77 K. However, in the present investigation the reduction of

---

(25) Narayana, P. A.; Suryanarayana, D.; Kevan, L. *J. Am. Chem. Soc.* **1982**, *105*, 3552.

O_2 to O_2^- at a platinum electrode has been found to be 27% efficient and at a graphitic carbon electrode 67% efficient.

Only with the utmost care can stable solutions of $[(Me_4N)O_2]_2$ and its monomer be prepared in dry MeCN. Water contents that are greater than 20 ppm (1 mM) cause the dimer to dissociate rapidly to the monomer and cause the latter to decompose (see eq 4). Furthermore, the presence of trace metals in the solvents, the reagents, and the glassware surfaces, even at ppb levels, rapidly decomposes $(Me_4N)O_2$ as well as other sources at O_2^-; this is especially evident in MeCN, which only weakly solvates O_2^-. For example, the use of quartz 1-mm spectrophotometric cells that have not been scrupulously cleaned with ammoniacal EDTA solution will cause a 0.5 mM $(Me_4N)O_2$ solution to have an apparent molar absorptivity that is only 15–25% of the value obtained with metal-free cells.

The remarkable stability of $(Me_4N)O_2$ solutions in 90%:10% H_2O/MeCN (0.1 M $(Me_4N)OH$) must be due to the selective solvation of $HO_2\cdot$ (the primary hydrolysis product of O_2^-). Bielski[14] has used pulse radiolysis studies to determine the disproportionation rate constants for O_2^- in aqueous media (eq 6–8).

$$H^+ + O_2^- \rightleftharpoons HO_2\cdot \qquad pK_a = 4.69 \tag{6}$$

$$O_2^- + HO_2\cdot \rightarrow O_2 + HO_2^- \qquad k_7 = 1.0 \times 10^8\ M^{-1}\ s^{-1} \tag{7}$$

$$\begin{gathered} HO_2\cdot + HO_2\cdot \rightarrow O_2 + H_2O_2 \\ k_8 = 8.5 \times 10^5\ M^{-1}\ s^{-1} \end{gathered} \tag{8}$$

Addition of excess acid to $(Me_4N)O_2$ in 90%:10% H_2O/MeCN results in rapid disproportionation to H_2O_2 and O_2; the apparent rate is consistent with eq 8:[26]

$$\begin{gathered} (MeCN)HO_2\cdot + (MeCN)HO_2\cdot \rightarrow \\ [(MeCN)(HO_2)_2(MeCN)] \rightarrow 2MeCN + H_2O_2 + O_2 \end{gathered} \tag{9}$$

For the conditions of 0.1 M OH^- in an aqueous solution, reaction 7 indicates that 1 mM O_2^- has a half-life at room temperature of about 15 min. However, when the solution contains 10% MeCN, 0.5 mM $(Me_4N)O_2$ only decays 10–15% during a 15-h period. This can be rationalized if the mechanism for aqueous disproportionation involves a proton bridge to facilitate electron transfer (H atom transfer):

$$O_2^- + HO_2\cdot \rightarrow [\cdot O_2^- {-} H^+ {-} O_2^- \cdot] \rightarrow O_2 + HO_2^- \tag{10}$$

Solvation of $HO_2\cdot$ by MeCN (to give $(MeCN)HO_2\cdot$) would hinder this pathway and retard its rate sufficiently to cause reaction 9 to be the limiting process. The half-life of 0.5 mM $(Me_4N)O_2$ in 90%:10% H_2O/MeCN (0.1 M $(Me_4N)OH$) is estimated to be about 10^6 h if the rate constant of eq 8 is assumed to control the disproportionation.

For many applications electrosynthesis of O_2^- by reduction of dissolved O_2 in aprotic solvents (with tetraalkylammonium salts as supporting electrolytes) is a more convenient and reliable approach. The same is true for the use of 18-crown-6 ether to enhance the solubility of KO_2 in nonaqueous solvents. Because KO_2 is significantly soluble in Me_2SO (1.3 mM) and DMF (0.3 mM), it remains the most useful and convenient source for many studies of the chemical reactivity for O_2^-. (With 0.1 M tetraethylammonium perchlorate present, the solubility of KO_2 in Me_2SO increases to 5.4 mM; probably by metathesis, $KO_2(s) + (Et_4N)ClO_4 \rightarrow (Et_4N)O_2 + KClO_4(s)$.)

Acknowledgment. This work was supported by the National Science Foundation under Grant No. CHE79-22040 and by the National Institutes of Health–USPHS under Grant No. GM-22761. We are grateful to Professor C. S. Foote and Dr. H. J. Guiraud (Department of Chemistry, University of California, Los Angeles) for helpful advice and assistance with the optimization of the synthetic procedures for $(Me_4N)O_2$, to Professor D. F. Bocian and G. A. Schick of this department for assistance with the Raman spectroscopic measurements, and to Dr. Subhash Harmalker of this department for assistance with the ESR measurements.

Registry No. KO_2, 12030-88-5; $(Me_4N)OH\cdot 5H_2O$, 10424-65-4; $(Me_4N)O_2$, 3946-86-9.

---

[26] Although a mechanism that involves HOOOOH as the activated complex is appealing, acidification of a Me_2SO solution that contains a 50:50 mixture of $^{16}O_2^-$ and $^{18}O_2^-$ yields a 50:50 mixture of $^{16}O_2$ and $^{18}O_2$ and negligible $^{16}O^{18}O$. (If HOOOOH were the major intermediate, a 50% yield of $^{16}O^{18}O$ would be expected.) Hence, the proton-induced disproportion of O_2^- in solution must occur via the same mechanism as that for $HO_2\cdot$ in the gas phase:[27]

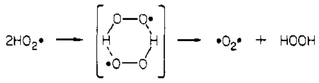

[27] Giguère, P. A. *J. Phys. Chem.* **1981**, *85*, 3733.